

We are IntechOpen, the world's leading publisher of Open Access books Built by scientists, for scientists

6,900

Open access books available

186,000

International authors and editors

200M

Downloads

Our authors are among the

154

Countries delivered to

TOP 1%

most cited scientists

12.2%

Contributors from top 500 universities



WEB OF SCIENCE™

Selection of our books indexed in the Book Citation Index
in Web of Science™ Core Collection (BKCI)

Interested in publishing with us?
Contact book.department@intechopen.com

Numbers displayed above are based on latest data collected.
For more information visit www.intechopen.com



Quantum Optics Phenomena in Synthetic Opal Photonic Crystals

Vasilij Moiseyenko and Mykhailo Dergachov
Oles' Honchar Dnipropetrovsk National University
Ukraine

1. Introduction

Optical phenomena in materials with a space modulation of dielectric constant at distances close to the light wavelengths (so called photonic band-gap structures or photonic crystals) are of a great interest now because of the existence of band gaps in their photonic band structure (Bykov, 1972; Yablonovitch, 1987; John, 1987). These band gaps represent frequency regions where electromagnetic waves are forbidden, irrespective of the spatial propagation directions. Inside the band gaps, the photon density of states is equal to zero and so the emission of light sources embedded in these crystals should be inhibited in these spectral regions (Vats et al., 2002). Since the time the effect is predicted, many experiments have been devoted to studies of spontaneous emission of molecules embedded in photonic crystals (Gaponenko et al., 1999; Gorelik, 2007). Typical structures of photonic crystals and calculations of corresponding photonic band structures are presented in a book by Prof. Joannopoulos (Joannopoulos et al., 2008). Besides the emission inhibition effect, a number of new optical phenomena in 3D photonic crystals, interesting from the applied point of view, are under intensive study now. The main research directions are the following:

- Effects of light localisation (John, 1987; Kaliteevskii et al., 2005; Vignolini et al., 2008).
- Radiation of photonic crystals filled with organic (rhodamine 6G, 1,8-naphthoylene-1',2'-benzimidazole, stilbene) and inorganic (ZnO, ZnS, rare-earth ions Eu^{3+} , Tb^{3+} , Er^{3+}) luminophores near by the edges of photonic band-gap (Gaponenko et al., 1999; Aliev et al., 2002; Emel'chenko et al., 2005; Li et al., 2007).
- Radiation of CdTe, CdSe/ZnS quantum dots in photonic crystal volume (Gruzintsev et al., 2009; Ambrozevich et al., 2009).
- Quantum optics phenomena in nano-structured materials based on photonic crystals and nonlinear optical substances (Lin & Vuckovic, 2010).
- Effects of the radiation field amplification in photonic crystals (Lin & Vuckovic, 2010).
- Increase of solar cells efficiency with the use of photonic crystals (Florescu et al., 2007).

As a good prototype of 3D photonic crystals, synthetic opals made of $\alpha\text{-SiO}_2$ globules have been widely used (Gorelik, 2007). Diameter D of globules can be varied from 200 nm to 700 nm. Between globules there are tetrahedral and octahedral hollows (or pores) with a mean size of about $0.26D$. Synthetic opals are characterized by a stop-band or a pseudogap (i.e., a band gap actual for one direction) in the [111] direction and a singular behaviour of photon density of states near by the stop-band edges. The existence of pores in the opal structure

allows modifying optical properties of such systems by filling the pores with various substances.

Synthetic opal photonic crystals containing nonlinear optical substances give a good chance to observe quantum optics phenomena in spatially nonuniform media where the photon mean free path is close to the light wavelength. Moreover, in this case the input optical power that is necessary to observe phenomena may be lower than the power required usually for observing the same phenomena in uniform nonlinear substances. The reason for it is the existence of diffuse transfer of photons that can result in photon accumulating inside photonic crystals and, consequently, in local optical power increasing. In particular, the possibility of experimental manifestation of Raman scattering and spontaneous parametric down-conversion in synthetic opals is discussed (Gorelik, 2007). The latter phenomenon is of special interest as it is convenient method to obtain bi-photon fields consisting of correlated photon pairs (Kitaeva & Penin, 2005). In the recent years, crystals with chirped structure of quadratic susceptibility (Kitaeva & Penin, 2004), and materials with spatially regular and stochastic distribution of quadratic optical susceptibility (Kalashnikov et al., 2009), are considered as sources of bi-photons. It is quite possible synthetic opal photonic crystals will be ranked with these sources.

2. Fundamentals of quantum optics phenomena in photonic crystals

Optical processes in nano-structured materials with a period close to the light wavelength are essentially different from those in bulk uniform media. It is due to the regularities of propagation of Bloch optical waves in such periodic structures ("photon confinement").

2.1 Luminescence

Consider the spontaneous emission transition in two-level system presented in Fig. 1.

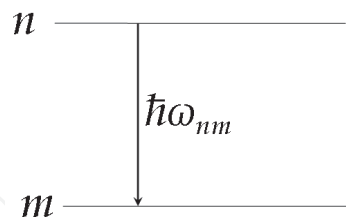


Fig. 1. Spontaneous emission transition in two-level system

The downward transition probability W_{nm} is determined in accordance with Fermi's golden rule as follows

$$W_{nm} = \frac{2\pi}{\hbar} \cdot \left| \langle m | \hat{H}_{\text{int}} | n \rangle \right|^2 \cdot g(E_n - \hbar\omega), \quad (1)$$

where $\left| \langle m | \hat{H}_{\text{int}} | n \rangle \right|$ is a matrix element of the perturbation operator, $g(E_n - \hbar\omega)$ is a density of final states of micro-object. In case of placing the micro-object into photonic crystal, the $g(E_n - \hbar\omega)$ spectrum is characterised by a density of optical states $g(\omega)$ in photonic crystal.

The spontaneous emission spectrum $S(\omega)$ is completely determined by the spectral distribution of transitions frequencies ω_{nm} and the density of optical states $g(\omega)$ within a region of these frequencies (Vats et al., 2002).

When frequencies ω_{nm} are in photonic band gap, where $g(\omega) = 0$, spontaneous emission must be completely inhibited. In general case, a dip in spontaneous emission spectrum should appear. The spectral position of this dip is correspondent to positions of reflection spectrum maximum and transmission spectrum minimum (Gaponenko et al., 1999). As a result of spontaneous emission inhibition the localisation of photon near by irradiative atom inside photonic crystal becomes possible if the transition frequency is within a band gap region or in the vicinity of band gap edges (John, 1987). In this case, bonded atom-photon state is coming into being. The photon emitted returns to the atom due to Bragg reflection and is re-absorbed by this atom. The existence of a group of such atoms may result in forming narrow photonic impurity band like an impurity band in semiconductor at sufficient concentrations of impurity atoms. Kinetics of luminescence in the vicinity of band gap edges demonstrates non-exponential behaviour (John, 1987).

2.2 Enhanced Raman scattering

Consider an elementary Stokes Raman scattering process as a disintegration of exciting photon ($\hbar\omega_{ex}, k_{ex}$) into scattered photon ($\hbar\omega', k'$) and optical phonon ($\hbar\Omega, K$) (Fig. 2).

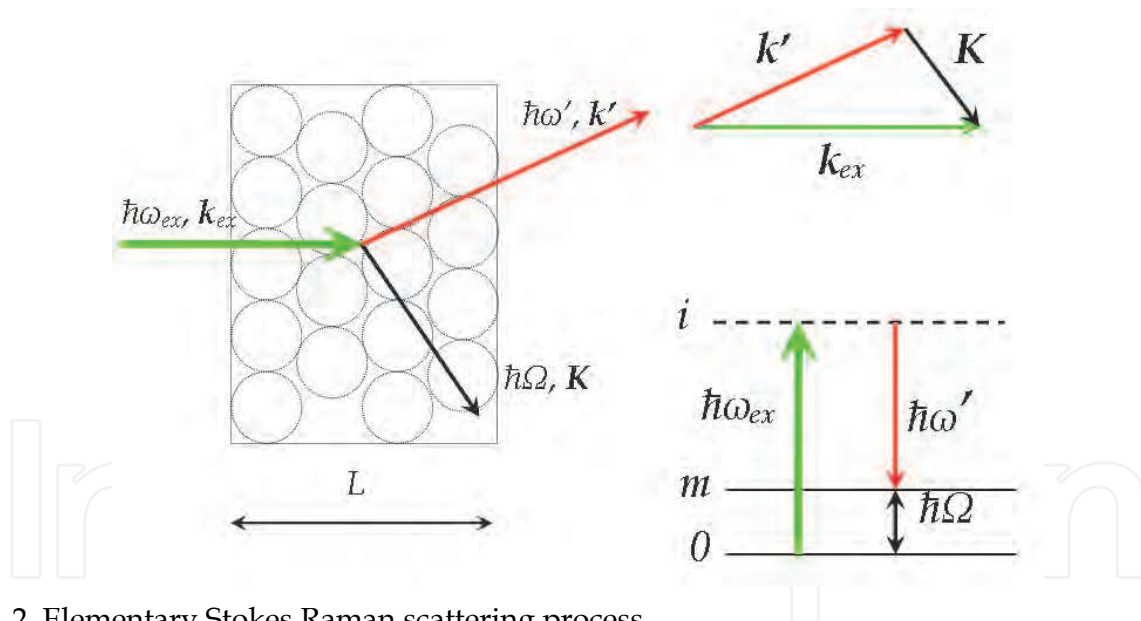


Fig. 2. Elementary Stokes Raman scattering process

The Stokes process probability $W(\omega')$ is determined by the density of optical states $g(\omega')$ in the region of scattered light frequencies (Poulet & Mathieu, 1970)

$$W(\omega') = \frac{2\pi}{\hbar} \cdot \left| \langle m | \hat{H}'_{int} | 0 \rangle \right|^2 \cdot g(\omega'), \tag{2}$$

where $\left| \langle m | \hat{H}'_{int} | 0 \rangle \right|$ is the modulus of the matrix element of the Hamiltonian of the radiation-substance interaction.

In general, the density of optical states $g(\omega)$ in photonic crystal is defined by a photon dispersion law and has maxima near by the band gap edges, where $(d\omega / dk) \rightarrow 0$. In the frame of one-dimensional model it can be determined as follows

$$g(\omega) = (k^2 / \pi^2)(d\omega / dk)^{-1}. \quad (3)$$

Exciting photons with the frequency ω_{ex} in the vicinity of band gap edges have the velocity values close to zero. It results in increasing the interval t'_{int} of radiation-substance interaction in photonic crystal compared with the interval t_{int} in uniform material, according to the following expression

$$t'_{int} = t_{int} \cdot \frac{c}{n_{eff}} \cdot (d\omega / dk)^{-1}, \quad (4)$$

where $c = 3 \cdot 10^8$ m/s and n_{eff} is an effective refractive index of photonic crystal. Besides, the interval t'_{int} may be enlarged because of the presence of "diffuse" photons whose motion is like to Brownian motion. Such diffuse photon transfer is most probably due to multiple photon reflections from disordered elements in photonic crystal structure. Both considered mechanisms give a reason to expect the enhancement of Raman scattering by substances infiltrated into photonic crystal.

2.3 Spontaneous parametric down-conversion

Spontaneous parametric down-conversion is a process of spontaneous disintegration of pump photons $(\hbar\omega_p, \mathbf{k}_p)$ into pairs of signal $(\hbar\omega_s, \mathbf{k}_s)$ and idler $(\hbar\omega_i, \mathbf{k}_i)$ photons. As this process is a second-order nonlinear process it occurs in media with no inversion symmetry. In case of spatially uniform media with a non-zero second-order nonlinear susceptibility $\chi^{(2)}$ the energy and momentum conservation is as follows

$$\omega_p = \omega_s + \omega_i, \quad \mathbf{k}_p = \mathbf{k}_s + \mathbf{k}_i \quad (5)$$

In frequency-degenerated ($\omega_s = \omega_i = \omega_p / 2$) and collinear ($k_s = k_i = k_p / 2$) regime at equal polarization of photons in pair (i.e., signal and idler photons are identical) the spectrum of bi-photons is determined by the following expression (Kalashnikov et al., 2009)

$$J(\Omega_{bp}) \sim \left[\frac{\sin x}{x} \right]^2, \quad (6)$$

where $x = (L / 2) \cdot (d^2k / d\Omega_{bp}^2) \cdot \Omega_{bp}^2$, Ω_{bp} is a frequency turning out of $\omega_p / 2$, L is a sample length in the pump propagation direction.

For spatially nonuniform media with regular structures (photonic crystals) a periodic modulation of linear and nonlinear susceptibilities should be considered in general case. By taking into account the $\chi^{(2)}$ periodic modulation the bi-photons spectrum should be determined by an additive sum of single harmonics of $\chi^{(2)}$ susceptibility (Kitaeva & Penin, 2005). The spectrum of each of these harmonics is shifted relative to the spectrum in uniform medium, according to the following "quasi-synchronism" condition (see also Fig. 3)

$$\Delta k_m \equiv k_s + k_i + m q - k_p = 0, \quad (7)$$

where $m = 1, 2, 3 \dots$, and q is a vector of photonic crystal reciprocal lattice ($q = 2\pi/d$, d is a period of photonic crystal structure).

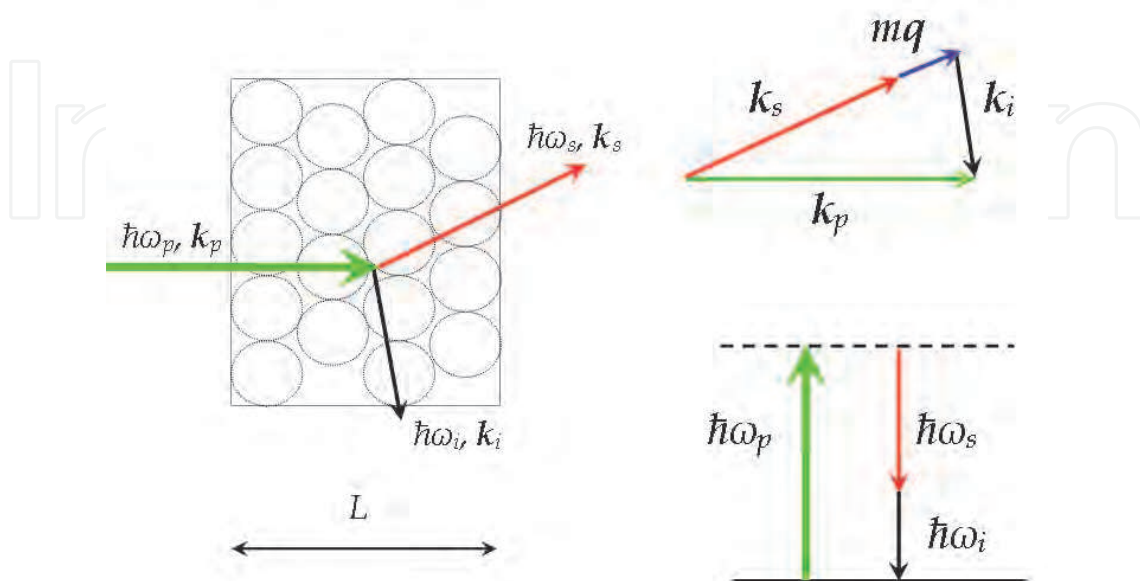


Fig. 3. Spontaneous parametric down-conversion process in photonic crystal

The intensity of each summand is determined by the square of magnitude of corresponding harmonic amplitude. An additional contribution to the parametric down-conversion spectrum should be given by interference of non-coinciding harmonics. At the absence of absorption the parametric down-conversion intensity $J_{\omega\Phi}$ per unit spectral $\Delta\omega$ and angular $\Delta\Phi$ intervals is determined by a magnitude of phase quasi-synchronism turning out Δ_m for the m -th order nonlinear diffraction (Kitaeva & Penin, 2004)

$$J_{\omega\Phi} \sim I_0 \cdot L^2 \sum_m \left| \chi_m^{(2)} \frac{\sin(\Delta_m / 2)}{(\Delta_m / 2)} \right|^2 \quad (8)$$

where I_0 is a pump intensity, $\chi_m^{(2)}$ is an amplitude of the m -th Fourier component of spatial distribution of nonlinear susceptibility $\chi^{(2)}$. The phase quasi-synchronism turning out Δ_m is defined via the phase synchronism turning out Δ in spatially uniform medium as follows

$$\Delta_m = \Delta - m q L. \quad (9)$$

In contrast to parametric down-conversion spectrum of spatially uniform sample the bi-photon field spectrum of photonic crystal should be broadened, and the interference effects may appear in its spectral intensity distribution (Kitaeva & Penin, 2004, 2005; Nasr et al., 2008; Kalashnikov et al., 2009). One of the reasons that cause an additional broadening of the bi-photon spectrum in photonic crystal is the presence of structure disordered domains with period d varied along a pump propagation direction. Besides, observable spectrum should be determined by the density of optical states $g(\omega)$ in the region of scattered light frequencies as a result of periodical modulation of linear susceptibility.

3. Characterisation of samples and experimental setup

Nanodisperse globules of silica dioxide were synthesized using a modified Stöber method (Stöber et al., 1968) through hydrolysis of tetraethoxysilane $\text{Si}(\text{OC}_2\text{H}_5)_4$ at high values of water concentration. Bulk synthetic opals were obtained by natural sedimentation of $\alpha\text{-SiO}_2$ globules with the following annealing of samples at 800°C during several hours. Annealing was performed in order to remove organic residua, extra- and intra-globular ethoxygroups, and chemically bound water (Samarov et al., 2006). Dimensions of obtained samples were about $1.0 \times 1.0 \times 0.2 \text{ cm}^3$.

Characterization of initial opals was performed by analyzing the surface structure with the use of X-Ray Microanalyzer JEO JXA 8200 and by measuring transmission and reflection spectra within a visible spectral range (Fig. 4, 5). Opal samples in these studies were composed of hexagonal close-packed layers of monodisperse $\alpha\text{-SiO}_2$ globules which are arranged in the face centred cubic lattice. The value of globules diameter D in various samples was from 250 nm to 270 nm, and the distance d between the (111) planes was from 204 nm to 220 nm.

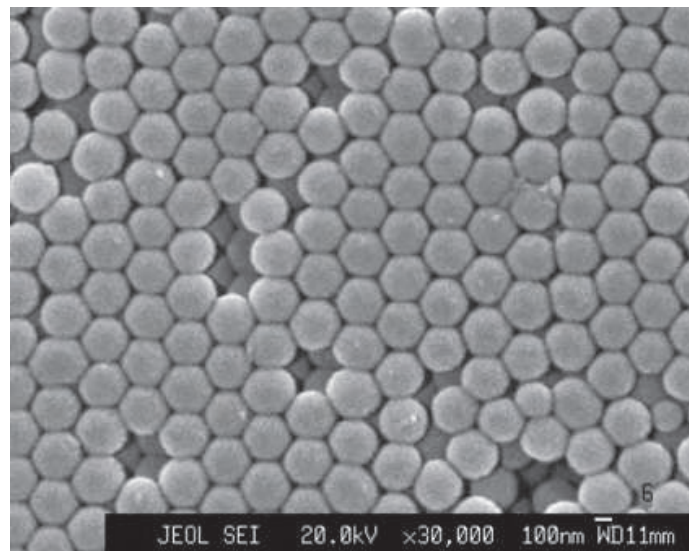


Fig. 4. Image of the opal surface in [111] direction. Diameter of globules $D = 270 \text{ nm}$

Parameters of photonic stop-band in [111] direction (spectral position of stop-band centre λ_c and its spectral width $\Delta\lambda_g$) were determined from transmission and reflection spectra as the parameters of non-transmission or reflection band (spectral position of maximum and spectral band width) formed in accordance with Bragg diffraction mechanism. The spectral position of reflection maximum (or transmission minimum) assigned as stop-band centre λ_c is dependent of an incident angle θ , effective refractive index n_{eff} and distance d between the (111) planes as follows (Podolsky et al., 2006):

$$\lambda_c(\theta) = 2d\sqrt{n_{eff}^2 - \sin^2 \theta} . \quad (10)$$

The effective refractive index n_{eff} is determined by the refractive index n_s of $\alpha\text{-SiO}_2$ globules ($n_s = 1.47$), the refractive index n_p of substance in opal pores (for initial opal it is air, $n_p = 1$) and the volume fraction f occupied by $\alpha\text{-SiO}_2$ globules (in our case, $f \approx 0.74$) as follows:

$$n_{eff}^2 = f \cdot n_s^2 + (1 - f) \cdot n_p^2. \quad (11)$$

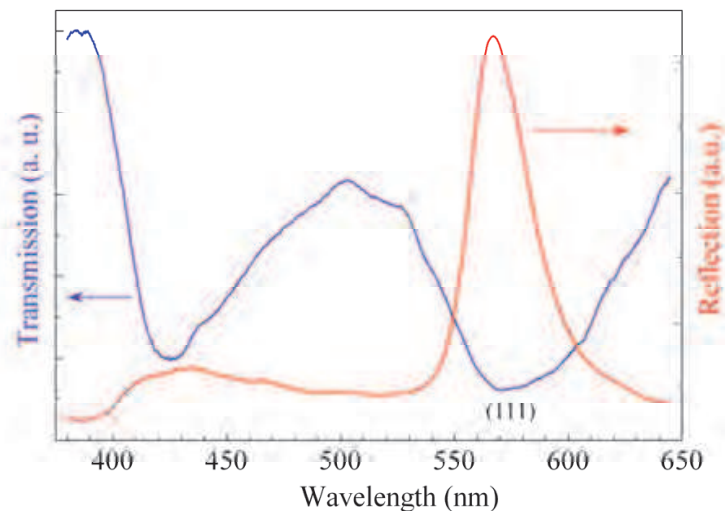


Fig. 5. Typical transmission and reflection spectra of initial opals ($D = 255$ nm). Transmission spectrum was measured at normal incidence to (111) plane ($\theta = 0^\circ$), reflection spectrum was measured at $\theta = 7^\circ$

Photonic crystals based on synthetic opals were obtained by further infiltration of initial opals with organic luminophores (rhodamine 6G, 2,5-bis(2-benzoxazolyl)hydroquinone, pironin G, astrofloksin) or nonlinear optical substances ($\text{Ba}(\text{NO}_3)_2$, LiIO_3 , KH_2PO_4 , $\text{Li}_2\text{B}_4\text{O}_7$). In most cases the infiltration was performed by a multiple soaking of samples in corresponding supersaturated solutions at room temperature. For example, synthetic opals were filled with rhodamine 6G by soaking samples in a dilute ethanol solution with laser dye concentrations of 10^{-4} M or $5 \cdot 10^{-3}$ M. After soaking the obtained samples were in the air until ethanol was evaporated. In case of infiltration with $\text{Ba}(\text{NO}_3)_2$, LiIO_3 , KH_2PO_4 an additional annealing of samples was performed at temperatures lower than melting ones (595 °C for $\text{Ba}(\text{NO}_3)_2$ and 120 °C for LiIO_3) to remove water. In case of $\text{Li}_2\text{B}_4\text{O}_7$ the initial opal was in $\text{Li}_2\text{B}_4\text{O}_7$ melt at 860 °C.

Reflection and transmission spectra of opals after infiltration were measured to prove the existence of corresponding substance in pores. Two types of changes in the spectra were registered. First, in opals with organic luminophores, an additional non-transmission band caused by absorption of embedded molecules was observed (Fig. 6). Second, the band caused by Bragg diffraction was shifted if a quantity of embedded substance was enough to change essentially the value of n_{eff} , according to expression (11) (Podolskyy et al., 2006).

In some experiments, in order to diminish (or exclude) the photonic stop-band effects and to study phenomena in a regular matrix of nano-emitters the opal samples were additionally soaked in water-glycerine solutions or pure glycerine. Opal infiltration with any water-glycerine solution yields in decreasing dielectric contrast in the synthetic opal photonic crystals as the refractive index of a water-glycerin solution n_p (variable from 1.39227 till 1.47399 in our experiments) is close to that of SiO_2 globules n_s . It causes the shift of the stop-band center λ_c to the longer wavelengths (10) and the narrowing of stop-band region $\Delta\lambda_g$ with increasing glycerin concentration.

For studying luminescence and light scattering phenomena in synthetic opals photonic crystals the incoherent and coherent light sources were used. The incoherent light sources were two light emitting diodes Edixeon EDST-3LAX ($\lambda = 400$ nm and 517 nm, $\Delta\lambda_{1/2} \approx 30$ nm, and the average power $P = 30$ mW). The coherent light sources were the pulsed nitrogen laser ($\lambda = 337$ nm, $\Delta\lambda_{1/2} = 0.1$ nm) with the pulse repetition frequency of 100 Hz and $P = 3$ mW, the semiconductor laser ($\lambda = 407$ nm, $\Delta\lambda_{1/2} = 1$ nm, $P = 60$ mW), and the diode-pumped solid state laser ($\lambda = 532$ nm, $\Delta\lambda_{1/2} = 1$ nm, $P = 120$ mW). As a rule, the forward and back scattering geometry along the [111] direction were used. Length of samples along the excitation direction was from 2 mm to 3 mm. Some experiments on light scattering were performed in the right angle geometry. The secondary emission from the sample surface was collected along the [111] direction by using lens with an aperture of about $0.17 \cdot \pi$ sr. The angular dependences of emission spectra were obtained within an angles region from 1° to 5° with the use of circle diaphragms. Spectral analysis was performed by using modernized spectrometer DFS-12. Signal registration was carried out in a regime of photon counting with accumulation.

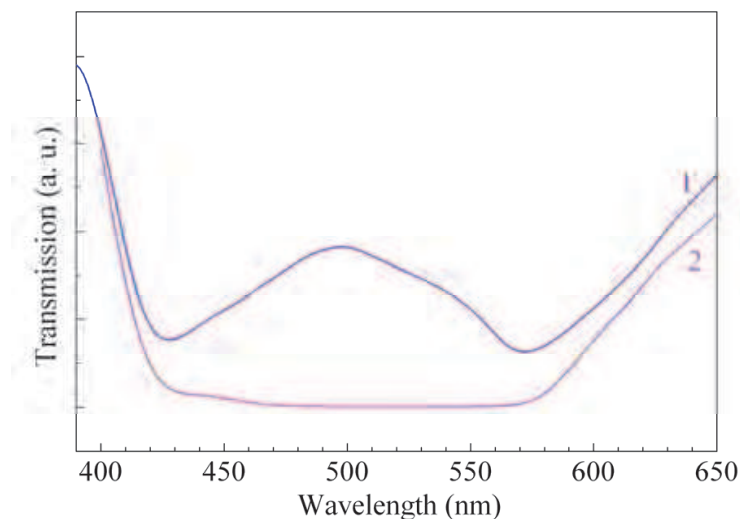


Fig. 6. Transmission spectra of initial opal (1) and the same opal infiltrated with pironin G (2). Spectra were measured at normal incidence to (111) plane ($\theta = 0^\circ$)

4. Results and discussion

In emission spectra of synthetic opal photonic crystals under optical excitation three typical regions are clearly observed (Gaponenko et al., 1999; Gorelik, 2007; Gruzintsev et al., 2008). One of them takes place in the opal-luminophores spectra, and is beyond doubt caused by the irradiative transitions between luminophore molecule levels. The other regions are inherent in emission spectra of opals filled with nonlinear optical substances. The first one is in a spectral range typical for Raman scattering region. The position of the second one is more distanced from an exciting line and is rather correlated with a stop-band position.

4.1 Luminescence of organic molecules in synthetic opals

As mentioned above synthetic opals are characterised by a presence of band gap in one space direction. This is why a complete inhibition of spontaneous emission should be

absent. Nevertheless, the use of opals as containers of emitting organic molecules allows changing the irradiative transitions probabilities remarkably (Bechger et al., 2005). It may be actual for substances with intra-molecular proton transfer, such as 2,5-bis(2-benzoxazolyl)hydroquinone, to control the probabilities of transitions with and without proton transfer.

4.1.1 Laser dyes molecules

Luminescence spectra of laser dyes (rhodamine 6G and pironin G) are shown in Fig. 7 (Moiseyenko et al., 2008, 2010). As seen from Fig. 7, for both molecules embedded into opal matrix a partial inhibition of luminescence intensity takes place within a region corresponding to the stop-band. For the rhodamine 6G spectrum, enhancement of the short-wavelength tail of the emission band is observed, while the long-wavelength tail of the spectrum is not altered essentially (Fig. 7, a). At the same time, the opal-pironin G spectrum is concentrated inside a long-wavelength region though it is rather not amplified (Fig. 7, b).

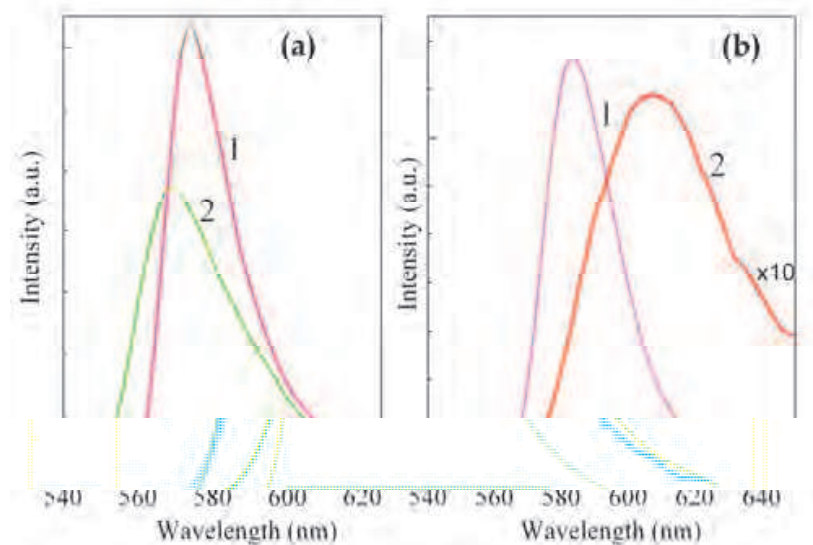


Fig. 7. Luminescence spectra of rhodamine 6G (a) and pironin G (b) put into optical cell with an ethanol (1) and infiltrated into opals (2) at a 517 nm diode excitation. Rectangles point to stop-band positions.

Following Bechger et al., 2005, observed transformations may be explained in such a way. When the light with wavelength λ_{em} shorter than a stop-band centre λ_c is emitted in the [111] direction it encounters Bragg diffraction at higher angles. Because of diffuse propagation more light is detected in the [111] direction at these higher angles. For the light of any longer wavelengths ($\lambda_{em} > \lambda_c$) all the directions in opal volume are equivalent and that light escapes the sample without being enhanced. As mentioned above, spectral distribution of spontaneous emission is defined by density of photon states $g(\omega)$. In both cases the spectral intensity maximum is near by the stop-band edge where the density of states $g(\omega)$ has maximum (Fig. 7). An absence of total inhibition inside stop-band region can be connected with a structure disorder that results in appearance of local states in the stop-band (Kaliteevskii et al., 2005). From these points of view luminescence spectra of rhodamine 6G and pironin G in opals with additional water-glycerine solutions (Fig. 8) may be interpreted

as follows. Infiltration with any water-glycerine solution results in lowering dielectric contrast. It causes a shift of stop-band centre λ_c to longer wavelengths. In accordance with our calculations by using expressions (10, 11), the stop-band shift is equal to 6 nm by varying glycerine volume concentration from 66 % till 100 %. It corresponds exactly to the luminescence maximum shift observed in the opal-rhodamine 6G spectrum (Fig. 8, a). In case of pironin G, we have somewhat different behaviour (Fig. 8, b, and Fig. 9).

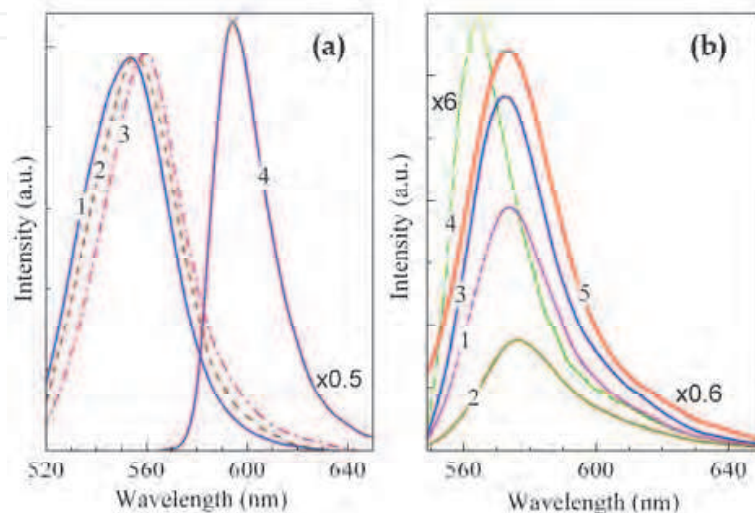


Fig. 8. Luminescence spectra of rhodamine 6G (a) and pironin G (b) placed into opals filled with a water-glycerin solution and in the optical cell with pure glycerine. In case (a) glycerine volume concentrations are 66 % (1), 75 % (2), 100 % (3), and curve 4 is the spectrum in pure glycerine. In case (b) glycerine volume concentrations are a 40% (1), 60% (2), 80% (3), 100% (4), and curve 5 is the spectrum in pure glycerine.

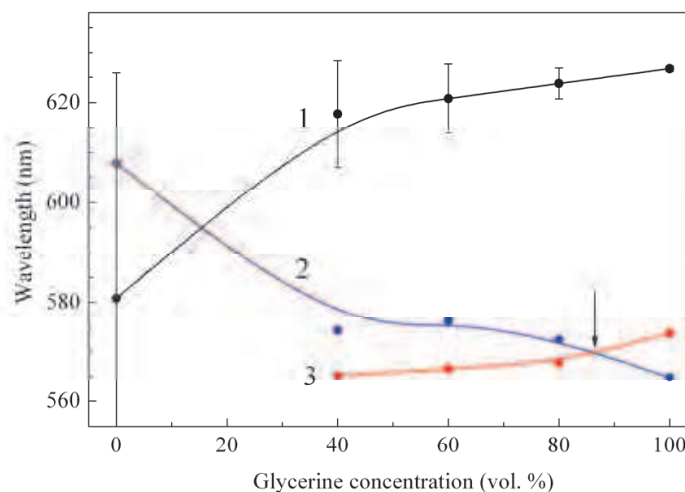


Fig. 9. Concentration dependences of stop-band center λ_c (1), pironin G luminescent maxima in opals (2) and water-glycerine solution in optical cell (3). The bars are stop-band widths.

Without infiltrating opals with a solution the condition $\lambda_{em} > \lambda_c$ takes place and we have a weak emission in the long-wavelength region discussed above (Fig. 7, b). By increasing glycerine concentration the relation between λ_{em} and λ_c becomes the opposite ($\lambda_{em} < \lambda_c$) and

the short-wavelength tail of the luminescence band is being enhanced. At glycerine concentrations close to 85 volume per cents (marked by the arrow in Fig. 9), the dielectric contrast vanishes ($\Delta\lambda_g = 0$) and luminescent band position becomes just the same as in the optical cell (a so-called solvent effect). After passing through this concentration, the stop-band width $\Delta\lambda_g$ starts growing due to increasing refractive index n_p . In this case we have an inversion of photonic bands, something like that occurring in narrow-gap semiconductors. The luminescent band in such inverse opal is shifting towards a “blue” side.

4.1.2 Intra-molecular proton transfer substances

2,5-bis(2-benzoxazolyl)hydroquinone belongs to a class of substances that manifests intra-molecular excited-state proton transfer. This substance is tautomerized in the conditions of ultraviolet excitation and shows a pronounced luminescence in green-red region with a large Stokes shift. When 2,5-bis(2-benzoxazolyl)hydroquinone in a hexane solution is excited within a main absorption band (280 nm – 420 nm), the irradiative transitions in both structural forms appear the spectrum (curve 1 in Fig. 10). The band in the 430 nm – 470 nm region is correspondent to the transitions without proton transfer, the band in the 580 nm – 620 nm region is due to the transitions with proton transfer. In condensed states these bands may be shifted towards the greater wavelength region. Thus a wide intensive band observed in the polycrystalline state spectrum within a 600 nm – 750 nm region is a result of the shift of a “proton-transfer” band. A shoulder of this band (in the 490 nm – 560 nm region) is most likely due to the impurity luminescence. It is proved by diminishing this band intensity in amorphous state (impurity-free state, according to our obtaining procedure) and by results presented by Chayka et al., 2005.

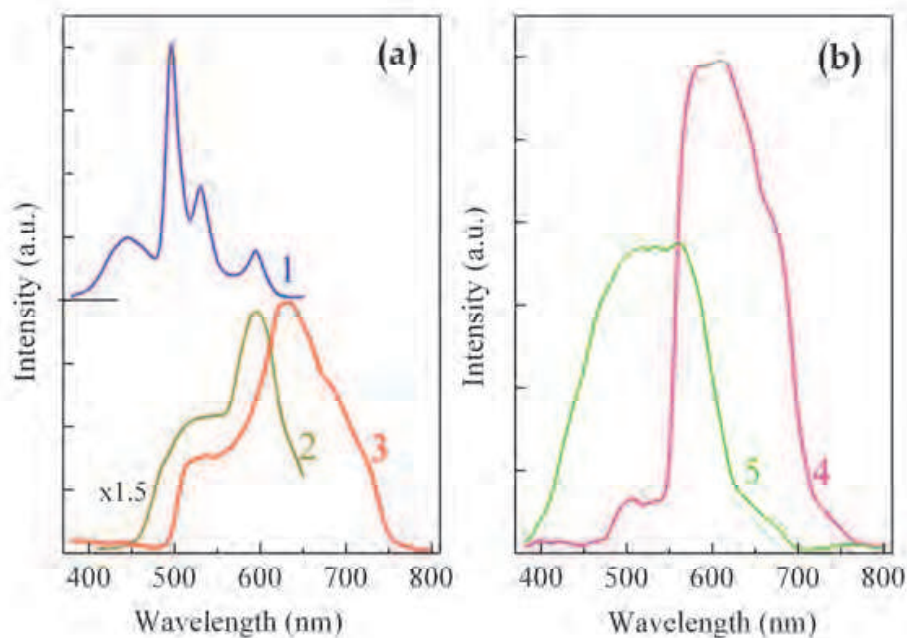


Fig. 10. Luminescence spectra of 2,5-bis(2-benzoxazolyl)hydroquinone in a hexane solution at a 400 nm diode excitation (1), in polycrystalline state at a 350 nm wide-band mercury lamp excitation (2), in polycrystalline (3) and amorphous (4) states, and into synthetic opal volume (5) at a 337 nm nitrogen laser excitation.

Spectral intensity distribution in the spectrum of 2,5-bis(2-benzoxazolyl)hydroquinone in synthetic opal is like to that in amorphous state (curves 4, 5 in Fig. 10). It allows assuming amorphous state of the substance in opal pores. The “blue” shift observed in this case may be explained in the following way. As a “proton-transfer” band is near by the stop-band region (600 nm – 640 nm in opal under study), the probability of these transitions decreases. It may result in increasing probabilities of impurity irradiative transitions and transitions without proton transfer. The latter transitions have not been observed in a “free” condensed state (Chayka et al., 2005). Another reason to make these processes observable is an accumulation of the shorter wavelength radiation because of Bragg reflection from the {111} planes at higher incident angles (Bechger et al., 2005).

4.2 Light scattering by synthetic opals filled with nonlinear optical dielectrics

Emission spectrum of synthetic opals with dielectrics observed within a wide spectral region under ultraviolet excitation may be divided into two parts. The first part is the spectrum located in the vicinity of the excitation line. The second one is in a region of 440 nm – 650 nm including a stop-band. By now the secondary emission of initial and dielectrics infiltrated opals has been given no universal explanation which should be satisfied by all experimental facts (Gorelik, 2007; Gruzintsev et al., 2008; Moiseyenko et al., 2009a, 2009b, 2012).

4.2.1 Enhanced spontaneous Raman scattering

Consider a total emission spectrum of initial synthetic opals; some of them were in air for a long time. The others were excited just after high temperature annealing. In all spectra a quite intensive band in the vicinity of the excitation line was observed. Its spectral position was independent of the stop-band position and previous technology conditions (Fig. 11). In the spectrum of a long time air-conserving sample a wide band with maximum at 570 nm was also observed. The fact that the band has vanished after annealing, i.e. after removing water in opal pores, reveals the impurity OH-groups luminescence origin of this band.

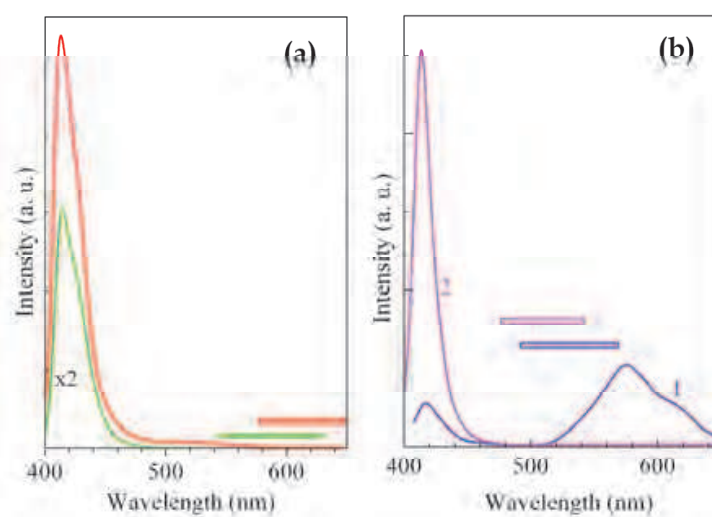


Fig. 11. Emission spectra of two different initial opals after thermal annealing at 800 °C (a). Emission spectra of opal conserved for a long time in the air at 70 % moisture (b) before (1) and just after (2) annealing at 700 °C. The rectangles point to the stop-band positions.

In order to understand the nature of the band near by the excitation line an influence of infiltrated substance on the emission spectrum has been studied (Moiseyenko et al., 2009a, 2009b). These spectra measured under spectral correct conditions with a 2 cm^{-1} resolution are presented in Raman shift scale after subtracting excitation line profile (Fig. 12, a). As seen from Fig. 12, spectral intensity distribution is dependent of kind of substance into opal pores. This fact together with mentioned above regularities allows us to suppose that the band observed within a typical vibrational spectrum range is caused by Raman scattering in substances forming photonic crystal. Such process becomes possible to be detected owing to an essential increase of field due to a slow diffuse motion of exciting photons into opal volume, and also, as a result of surface enhanced conditions inside opal pores.

However, obtained spectra are too wide compared with the usual Raman spectra. It may be explained, if remember, that band spectral profile is determined by spectral profile of excitation line and Raman spectrum of substance. In our initial experiments we have used a source with a significant width of the exciting line ($\Delta\lambda_{1/2} \approx 30 \text{ nm}$). Another reason for spectrum broadening is a possible amorphous state of substances which form the sample structure. In case of amorphous state, a density of vibrational states $g(\Omega)$ can be quantitatively described by calculating reduced Raman spectrum $J_R(\Omega)$ for the Stokes component (Cardona, 1975) (Fig. 12, b).

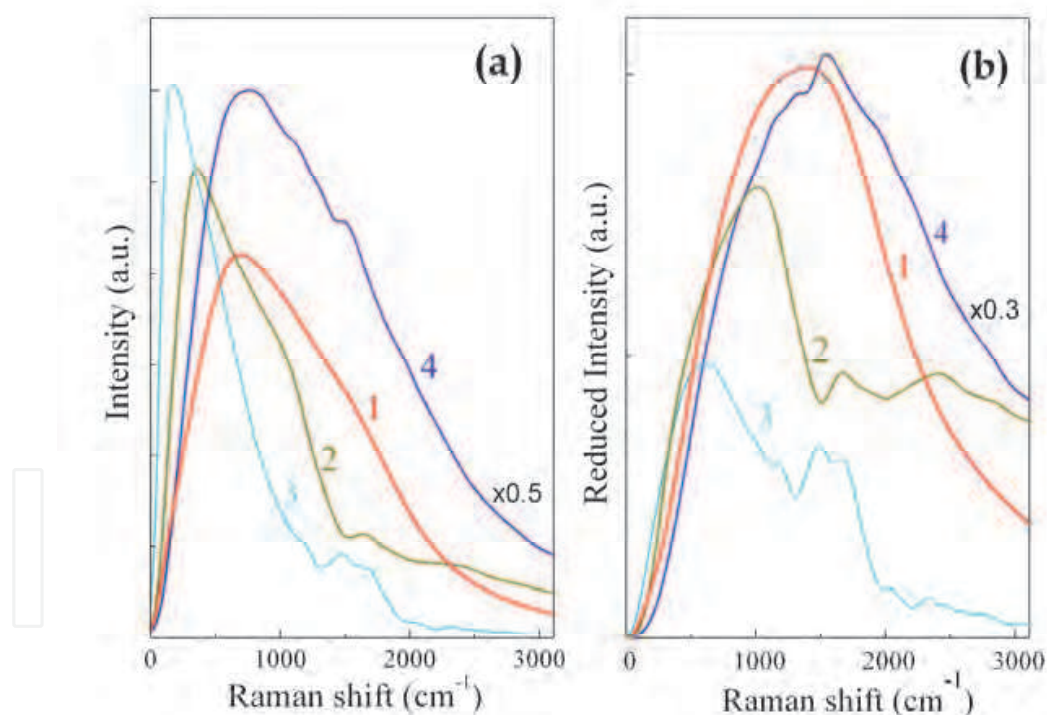


Fig. 12. Emission spectra (a) in the vicinity of the 400 nm exciting line and the corresponding reduced Raman spectra (b) for initial synthetic opal (1) and opals infiltrated with CuCl_2 (2), $\text{Ba}(\text{NO}_3)_2$ (3), and LiIO_3 (4)

To diminish a role of exciting radiation parameters in forming measured spectrum, we have used a 532 nm laser radiation with $\Delta\lambda_{1/2} \approx 1 \text{ nm}$ to excite emission in opal filled with KH_2PO_4 (Fig. 13). The significant band width in this case may testify amorphous state of substance in opal pores. The presence of the anti-Stokes component should be pointed out.

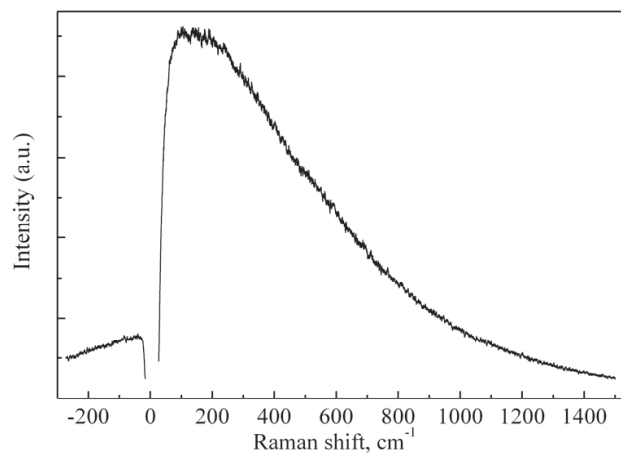


Fig. 13. Emission spectrum in the vicinity of the 532 nm laser exciting line for synthetic opal infiltrated with KH_2PO_4

The emission spectral distribution typical for Raman spectrum was observed in the opal- $\text{Li}_2\text{B}_4\text{O}_7$ spectrum in the right angle geometry (Fig. 14). The $A_1(\text{TO})$ Raman $\text{Li}_2\text{B}_4\text{O}_7$ spectrum measured earlier (Moiseyenko et al., 2006) at the excitation of a 532 nm Q-switched Nd:YAG laser with mean power of 250 mW is also presented in Fig. 14.

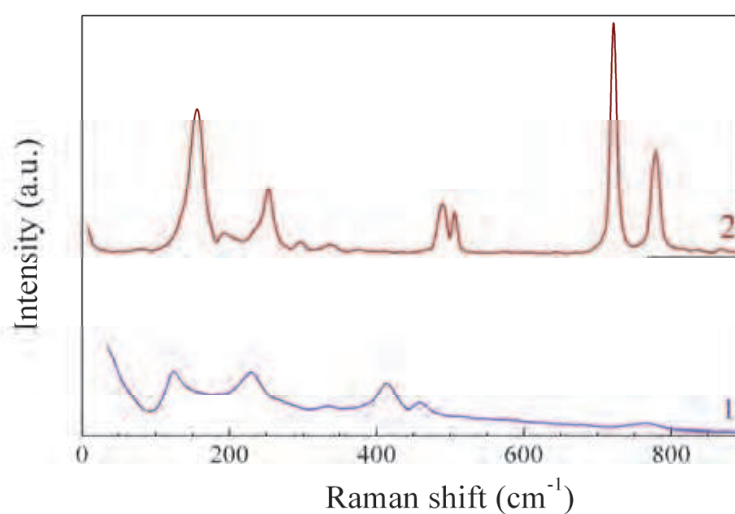


Fig. 14. The emission spectrum of opal infiltrated with $\text{Li}_2\text{B}_4\text{O}_7$ (1) and $A_1(\text{TO})$ Raman $\text{Li}_2\text{B}_4\text{O}_7$ spectrum (2) at the 532 nm laser excitation

Both spectra have a similar structure in the $100 \text{ cm}^{-1} - 550 \text{ cm}^{-1}$ spectral range, but the bands in the opal- $\text{Li}_2\text{B}_4\text{O}_7$ spectrum are shifted towards the excitation line and have a greater halfwidth. However, the values of bands halfwidths (no more than 30 cm^{-1}) give no reason to conclude amorphous state of the substance in opal pores. The broadening of bands is rather caused by structural disordering and the existence of polydomain structure. The bands shifts are most probably due to the small sizes of the unit $\text{Li}_2\text{B}_4\text{O}_7$ scattering volume defined by the pores sizes (no more than 100 nm in our samples). The coincidence of high-frequency Raman range and the stop-band spectral region results in a crucial decrease of emission intensity at Raman shifts higher than 600 cm^{-1} .

In order to experimentally prove the enhancement effects in synthetic opal photonic crystals Raman spectra in opal- $\text{Li}_2\text{B}_4\text{O}_7$ and single $\text{Li}_2\text{B}_4\text{O}_7$ crystal were measured in the low-frequency region under the same conditions (Fig. 15). As seen from Fig. 15, integral scattering intensity in the opal- $\text{Li}_2\text{B}_4\text{O}_7$ spectrum is about of a three times higher than the one in the single $\text{Li}_2\text{B}_4\text{O}_7$ crystal spectrum. Taking into account the lesser quantity of lithium tetraborate in opal matrix in the same scattering volume (no more than 26 % from total volume, as lithium tetraborate is situated only in opal pores) we can estimate the Raman enhancement coefficient as high as 10. Two enhancement mechanisms can be proposed. The first one is a photon slowing in accordance with a dispersion law in photonic crystals and the second is a multiple reflection from disordered planes resulting to diffuse photon motion (Gorelik, 2007).

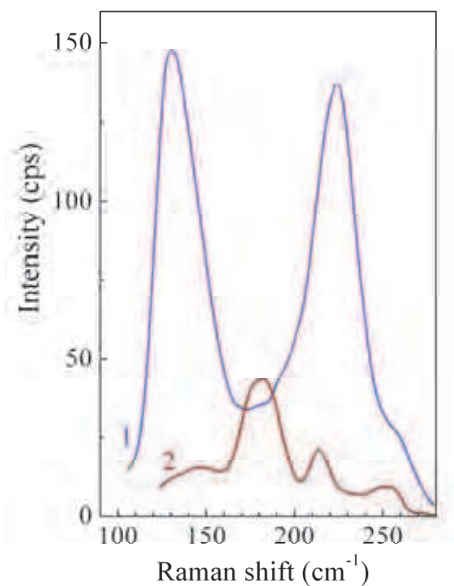


Fig. 15. Low-frequency region in non-polarised Raman spectra of opal infiltrated with $\text{Li}_2\text{B}_4\text{O}_7$ (1) and single $\text{Li}_2\text{B}_4\text{O}_7$ crystal (2) under the same conditions at the 532 nm diode pumped solid state laser excitation. The right angle geometry was used. The longer wavelength tale of excitation line was subtracted.

4.2.2 Spontaneous parametric down-conversion

Emission spectra of photonic crystals infiltrated with any nonlinear optical substances mentioned above are similar after subtracting the longer wavelength tale of excitation line and the bands corresponding to Raman scattering processes (Fig. 16). The spectra contain a wide asymmetric band within a 410 – 600 nm range. This band spectral position is different for opals with different infiltrators but it is correlated with the stop-band position. The emission intensity decreases within a stop-band region but it does not vanish completely because of the existence of point defects and structural disordering in photonic crystals.

Photos of secondary emission made far from sample surface reveal the angular distribution of spectral intensity (Moiseyenko et al., 2009b). Emission spectra measured at different scattering angles and treated by subtracting the longer wavelength tale of excitation line and

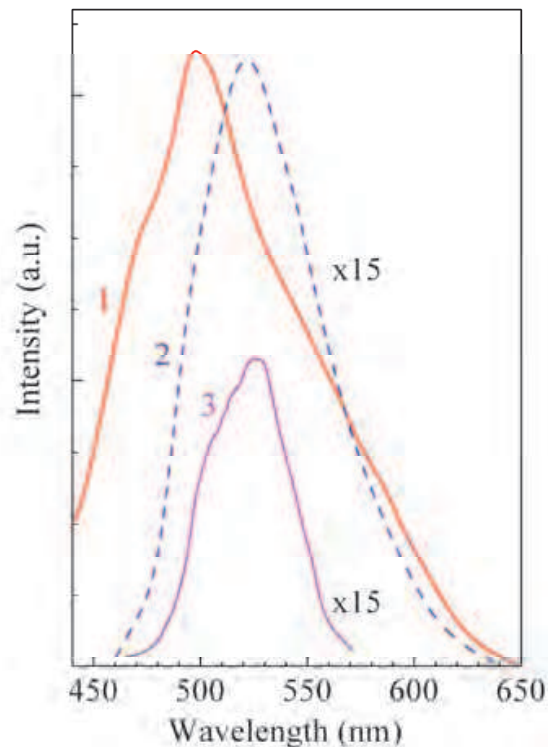


Fig. 16. Emission spectra of opals infiltrated with $\text{Ba}(\text{NO}_3)_2$ (1), LiIO_3 (2), and KH_2PO_4 (3) at a 400 nm diode excitation in the forward scattering geometry. Spectral stop-band positions are 525 nm – 590 nm (1), 560 nm – 615 nm (2, 3).

bands in Raman scattering region are presented in Fig. 17 (Moiseyenko et al., 2012). The spectral intensity distribution and the emission maximum position are quite different at various scattering angles. When dielectric contrast becomes negligible (by infiltrating opal with pure glycerine) a shifted symmetric emission band is observed (curve 4 in Fig. 17). In this case the sample may be considered as practically transparent matrix with periodic distributed nonlinear substance which is responsible for generating secondary emission. The symmetric form of spectral distribution is typical for spontaneous parametric down-conversion in uniform media (Kitaeva & Penin, 2005).

Thus, all elicited regularities together with chosen conditions of the samples heat treatment (Samarov et al., 2006) are the reasons to exclude the fluorescence of nano-composite components and the OH-groups fluorescence observed in synthetic opals within a 520 nm – 650 nm range (Gruzintsev et al., 2008). Taking into account angular dependences of spectral intensity, the emission observed may be interpreted as spontaneous parametric down-conversion in spatially nonuniform nonlinear optical media. Additional contribution to the emission within a 407 – 437 nm region may be given by enhanced Raman scattering discussed above.

As shown earlier, spontaneous parametric down-conversion intensity per a unit angle and spectral interval is determined by the value of quasi-synchronism Δ_m for the m -th order nonlinear diffraction. In case of 3D photonic crystals based on synthetic opals this magnitude is defined by the structure disordering degree, the nonlinear substance filling

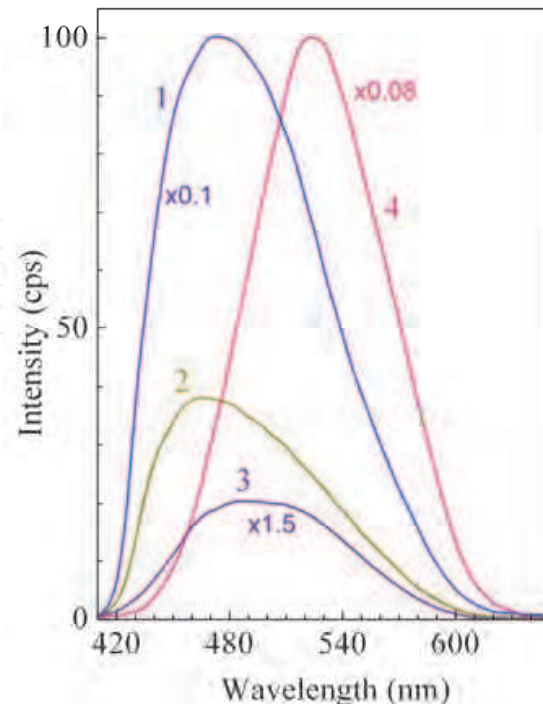


Fig. 17. Emission spectra of opal infiltrated with $\text{Ba}(\text{NO}_3)_2$ at a 407 nm laser excitation in the forward scattering geometry. The spectrum (1) was measured within a full angle range. The spectra (2) and (3) were registered at the angles of 5° and 3° to the pump propagation direction, respectively. The spectrum (4) was measured within a full angle range after additional sample infiltration with glycerine.

factor and by the existence of polydomain structure which forms additional superlattice. In our samples typical domain size was about of 70 mkm. Then the phase quasi-synchronism condition becomes true for the greater number of directions and wavelengths. It results in broadening the parametric down-conversion spectrum like that occurred in chirped structures with quadratic nonlinearity (Nasr et al., 2008). Besides spectrum broadening effects, nonlinear diffraction by 3D grating of quadratic optical susceptibility and bi-photon field interference may result in more complicated changes in spatial and frequency distribution of far field compared with that observed in polydomain crystals (Kitaeva & Penin, 2004).

5. Conclusion

In accordance with Fermi's golden rule, modification of luminescence spectra of organic molecules in synthetic opals is determined by the density of optical states in the vicinity of photonic stop-band. Inside stop-band region the partial inhibition of spontaneous emission is observed for all substances. If the wavelength, corresponding to the intensity maximum in spectrum of "free-state" substance, is shorter than wavelength, corresponding to the stop-band center, the amplification of dye luminescence at the high-energy edge of stop-band occurs. In the contrary case a weak luminescence is observed at the low-energy edge of stop-band without any amplifying.

The possibility of practical controlling probabilities of irradiative transitions without and with proton transfer by choosing properly the stop-band spectral position has been demonstrated. The “blue” shift of the luminescence spectrum of rhodamine 6G has been observed in opal additionally infiltrated with pure glycerine.

The emission band observed near by the exciting line is most probably due to Raman scattering in substances forming photonic crystal structure. It becomes possible to be detected owing to the essential increase of radiation field caused by the slow diffuse transfer of pump photons into sample volume.

Secondary emission of nonlinear photonic crystals under coherent and incoherent optical pumping observed within a 410 – 600 nm range has an asymmetric continual spectrum with a width of about 200 nm. The spectral intensity distribution and the intensity maximum position are dependent of the exciting radiation parameters (wavelength of excitation, degree of coherence, angle range of pumping wave vectors), of the emission detection angle, of the structure disordering degree. The emission observed is analyzed in terms of spontaneous parametric down-conversion phenomenon which occurs in spatially nonuniform nonlinear medium.

6. Acknowledgment

This work was financially supported by National Academy of Sciences of Ukraine, the Ukrainian-Russian project No.71-02-10 “Radiation of 3D photonic crystals under optical and electric excitations”.

7. References

- Aliev, G., Golubev, V., Dukin, A., Kurdyukov, D., Medvedev, A., Pevtsov, A., Sorokin, L., Hutchison, J. (2002). Structural, photonic band-gap, and luminescence properties of the opal-erbium composite. *Physics of the Solid State*, Vol.44, No12 (December 2002), pp. 2224-2231, ISSN 1063-7834
- Ambrozevich, S., Gorelik, V., Dirin, D., Vasil'ev, R., Vitukhnovsky, A., Voinov, Yu. (2009). Optical properties of 3D photonic crystals filled with CdSe/CdS quantum dots. *Journal of Russian Laser Research*, Vol.30, No4, (July 2009), pp. 384-391, ISSN 1071-2836
- Bechger, L., Lodahl, P., Vos, W. (2005). Directional fluorescence spectra of laser dye in opal and inverse opal photonic crystals. *Journal of Physical Chemistry B*, Vol.109, No5, (May 2005), pp. 9980-9988
- Bykov, V. (1972). Spontaneous emission in a periodic structure. *Soviet Physics - JETP (Journal of Theoretical and Experimental Physics)*, Vol.35, No.2, (February 1972), pp. 269-273, ISSN 0038-5646
- Cardona, M. (1975). *Light Scattering in Solids*, Springer-Verlag, Berlin
- Chayka, K., Moiseyenko, V., Mordzinski, A. (2005). Luminescence of 2,5-bis(2-benzoxazolyl)hydroquinone molecules adsorbed on copper island film. *Ukrainian Journal of Physical Optics*, Vol.5, No4 (November 2005), pp. 128-132, ISSN 1609-1833
- Emel'chenko, G., Gruzintsev, A., Koval'chuk, M., Masalov, V., Samarov, E., Yakimov, E., Barthou, C., Zver'kova, I. (2005). Opal - ZnO nanocomposites: Structure and

- emission properties. *Semiconductors*, Vol.39, No11, (November 2005), pp. 1328-1332, ISSN 1063-7826
- Florescu, M., Lee, H., Puscausu, I., Pralle, M., Florescu, L., Ting, D., Dowling, J.P. (2007). Improving solar cell efficiency using photonic band-gap materials. *Solar energy Materials & Solar Cells*, Vol.91, (June 2007), pp. 1599-1610, ISSN 0927-0248
- Gaponenko, S., Bogomolov, V., Petrov, E., Kapitonov, A., Yarotsky, D., Kalosha, I., Eychmuller, A., Rogach, A., McGlip, J., Woggon, U., Gindele, F. (1999). Spontaneous emission of dye molecules, semiconductor nanocrystals, and rare-earth ions in opal-based photonic crystals. *Journal of Lightwave Technology*, Vol.17, No.11, (November 1999), pp. 2128-2137, ISSN 0733-8724
- Gorelik, V., (2007). Optics of globular photonic crystals. *Quantum Electronics*, Vol.37, No5, (May 2007), pp. 409-432, ISSN 1063-7818
- Gruzintsev, A., Emel'chenko, G., Masalov, V., Romanelli, M., Barthou, C., Benalloul, P., Maitre, A. (2008). Luminescent properties of synthetic opal. *Inorganic materials*, Vol.44, No2, (February 2008), pp. 159-164, ISSN 0020-1685
- Gruzintsev, A., Emel'chenko, G., Masalov, V., Yakimov, E., Barthou, C., Maitre, A. (2009). Luminescence of CdSe/ZnS quantum dots infiltrated into an opal matrix. *Semiconductors*, Vol.43, No2, (February 2009), pp. 197-201, ISSN 1063-7826
- Joannopoulos, J., Johnson, S., Winn, J., Meade, R. (2008). *Photonic Crystals: Molding the Flow of Light* (second edition), Princeton University Press, ISBN 978-0-691-12456-8, Princeton and Oxford
- John, S. (1987). Strong localization of photons in certain disordered dielectric superlattices. *Physical Review Letters*, Vol.58, No23, (June 1987), pp. 2486-2489, ISSN 0031-9007
- Kalashnikov, D., Katamadze, K., Kulik, S. (2009). Controlling the spectrum of a two-photon field: Inhomogeneous broadening due to a temperature gradient. *JETP Letters*, Vol.89, No5, (May 2009), pp. 224-228, ISSN 0021-3640
- Kaliteevskii, M., Nikolayev, V., Abram, R., (2005). Eigenstate statistics and optical properties of one-dimensional disordered photonic crystals. *Physics of the Solid State*, Vol.47, No10, (October 2005), pp. 1948-1957, ISSN 1063-7834
- Kitaeva, G., Penin, A. (2004). Diagnostics of the inhomogeneous distribution of quadratic optical susceptibility over parametric scattering spectra. *Quantum Electronics*, Vol.34, No7, (July 2004), pp. 597-611, ISSN 1063-7818
- Kitaeva, G., Penin, A. (2005). Spontaneous parametric down-conversion. *JETP Letters*, Vol.82, No6, (September 2005), pp. 350-355, ISSN 0021-3640
- Li, M., Zhang, P., Li, J., Zhou, J., Sinitskii, A., Abramova, V., Klimonsky, S., Tretyakov, Y. (2007). Directional emission from rare earth ions in inverse photonic crystals. *Applied Physics B*, Vol.89, No2-3 (November 2007), pp. 251-255, ISSN 0946-2171
- Lin, Z., Vuckovic, J. (2010). Enhanced two-photon processes in single quantum dots inside photonic crystal nanocavities. *Physical Review B*, Vol. 81, No 035301, (January 2010), pp. 1-5, ISSN 1098-0121
- Moiseyenko, V., Dergachov, M., Burak, Ya. (2006). The influence of point defects on the vibrational spectrum of $\text{Li}_2\text{B}_4\text{O}_7$ crystal. *Ukrainian Journal of Physical Optics*, Vol.7, No.1, (March 2006), pp. 35-40, ISSN 1609-1833
- Moiseyenko, V., Guziy, O., Gorelik, V., Dergachov, M. (2008). Optically excited secondary emission spectra of photonic crystals based on synthetic opals. *Optics and spectroscopy*, Vol.105, No.6, (December 2008), pp. 919-923, ISSN 0030-400X

- Moiseyenko, V., Dergachov, M., Shvachich, V., Yevchik, A. (2009a). On the nature of the secondary emission of globular SiO₂ photonic crystals, *Proceedings of Metamaterials 2009 3rd International Congress on Advanced Electromagnetic Materials in Microwaves and Optics*, pp. 638-640, ISBN 978-0-9551179-6-1, London, UK, August 30 - September 4, 2009
- Moiseyenko, V., Dergachov, M., Shvachich, V., Yevchik, A. (2009b). The possibility for surface-enhanced Raman scattering and spontaneous parametric down-conversion by globular photonic crystals infiltrated with dielectrics. *Ukrainian Journal of Physical Optics*, Vol.10, No.4, (December 2009), pp. 201-205, ISSN 1609-1833
- Moiseyenko, V., Dergachov, M., Shvachich, V., Shvets, T., Roschenko, O. (2010). Spontaneous emission of laser dye molecules in synthetic opals under conditions of low dielectric contrast. *Ukrainian Journal of Physical Optics*, Vol.11, No.1, (March 2010), pp. 1-5, ISSN 1609-1833
- Moiseyenko, V., Dergachov, M., Shvachich, V. (2012). Spontaneous parametric light scattering in spatially inhomogeneous nonlinear media based on photonic crystals *Optics and spectroscopy*, Vol.112, No.2 (February 2012), pp. 198-200, ISSN 0030-400X
- Nasr, M., Carrasco, S., Saleh, B., Sergienko, A., Teich, M., Torres, J., Torner, L., Hum, D., Fejer, M. (2008). Ultrabroadband biphotons generated via chirped quasi-phase-matched optical parametric down-conversion. *Physical Review Letters*, Vol.100, No183601, (May 2008), pp. 1-4, ISSN 0031-9007
- Podolskyy, D., Moiseyenko, V., Gorelik V., Shvachich V. (2006). Reflection spectra of bare and infiltrated with Ba(NO₃)₂ synthetic opal photonic crystals. *Ukrainian Journal of Physical Optics*, Vol.7, No.2, (April 2006), pp. 58-62, ISSN 1609-1833
- Poulet, H., Mathieu, J.-P. (1970). *Spectres de Vibration et Symetrie des Cristaux*, Gordon & Breach Publishing Group, ISBN 0677501803, Paris - Londres - New York
- Samarov, E., Mokrushin, F., Masalov, V., Abrosimova, G., Emel'chenko, G. (2006). Structural modification of synthetic opals during thermal treatment. *Physics of the Solid State*, Vol.48, No.7, (July 2006), pp. 1280-1283, ISSN 1063-7834
- Stöber, W., Fink, A., Bohn, E. (1968). Controlled growth of monodisperse silica spheres in micron size range. *Journal of Colloidal and Interface Science*, Vol.26, No.2, (February 1968), pp. 62-68
- Vats, N., John, S., Busch, K. (2002). Theory of fluorescence in photonic crystals. *Physical Review A*, Vol.65, No043808, (March 2002), pp. 1-13, ISSN 1050-2947
- Vignolini, S., Riboli, F., Intonti, F., Belotti, M., Gurioli, M., Chen, Y., Colocci, M., Andreani, L., Wiersma, D. (2008). Local nanofluidic light sources in silicon photonic crystal microcavities. *Physical Review E*, Vol.78, No045603(R), (October 2008), pp. 1-4, ISSN 1539-3755
- Yablonoitch, E. (1987). Inhibited spontaneous emission in solid-state physics and electronics. *Physical Review Letters*, Vol.58, No20, (May 1987), pp. 2059-2062, ISSN 0031-9007



Quantum Optics and Laser Experiments

Edited by Dr. Sergiy Lyagushyn

ISBN 978-953-307-937-0

Hard cover, 180 pages

Publisher InTech

Published online 20, January, 2012

Published in print edition January, 2012

The book embraces a wide spectrum of problems falling under the concepts of "Quantum optics" and "Laser experiments". These actively developing branches of physics are of great significance both for theoretical understanding of the quantum nature of optical phenomena and for practical applications. The book includes theoretical contributions devoted to such problems as providing a general approach to describe electromagnetic field states with correlation functions of different nature, nonclassical properties of some superpositions of field states in time-varying media, photon localization, mathematical apparatus that is necessary for field state reconstruction on the basis of restricted set of observables, and quantum electrodynamics processes in strong fields provided by pulsed laser beams. Experimental contributions are presented in chapters about some quantum optics processes in photonic crystals - media with spatially modulated dielectric properties - and chapters dealing with the formation of cloud of cold atoms in magneto optical trap. All chapters provide the necessary basic knowledge of the phenomena under discussion and well-explained mathematical calculations.

How to reference

In order to correctly reference this scholarly work, feel free to copy and paste the following:

Vasilij Moiseyenko and Mykhailo Dergachov (2012). Quantum Optics Phenomena in Synthetic Opal Photonic Crystals, Quantum Optics and Laser Experiments, Dr. Sergiy Lyagushyn (Ed.), ISBN: 978-953-307-937-0, InTech, Available from: <http://www.intechopen.com/books/quantum-optics-and-laser-experiments/quantum-optics-phenomena-in-synthetic-opal-photonic-crystals>

INTECH
open science | open minds

InTech Europe

University Campus STeP Ri
Slavka Krautzeka 83/A
51000 Rijeka, Croatia
Phone: +385 (51) 770 447
Fax: +385 (51) 686 166
www.intechopen.com

InTech China

Unit 405, Office Block, Hotel Equatorial Shanghai
No.65, Yan An Road (West), Shanghai, 200040, China
中国上海市延安西路65号上海国际贵都大饭店办公楼405单元
Phone: +86-21-62489820
Fax: +86-21-62489821

© 2012 The Author(s). Licensee IntechOpen. This is an open access article distributed under the terms of the [Creative Commons Attribution 3.0 License](#), which permits unrestricted use, distribution, and reproduction in any medium, provided the original work is properly cited.

IntechOpen

IntechOpen